Opportunities and limits in imaging microorganisms and their activities in soil micro-habitats - figures

Védère Charlotte[a], Vieublé Gonod Laure[a], Nunan Naoise[b], Chenu Claire[a].

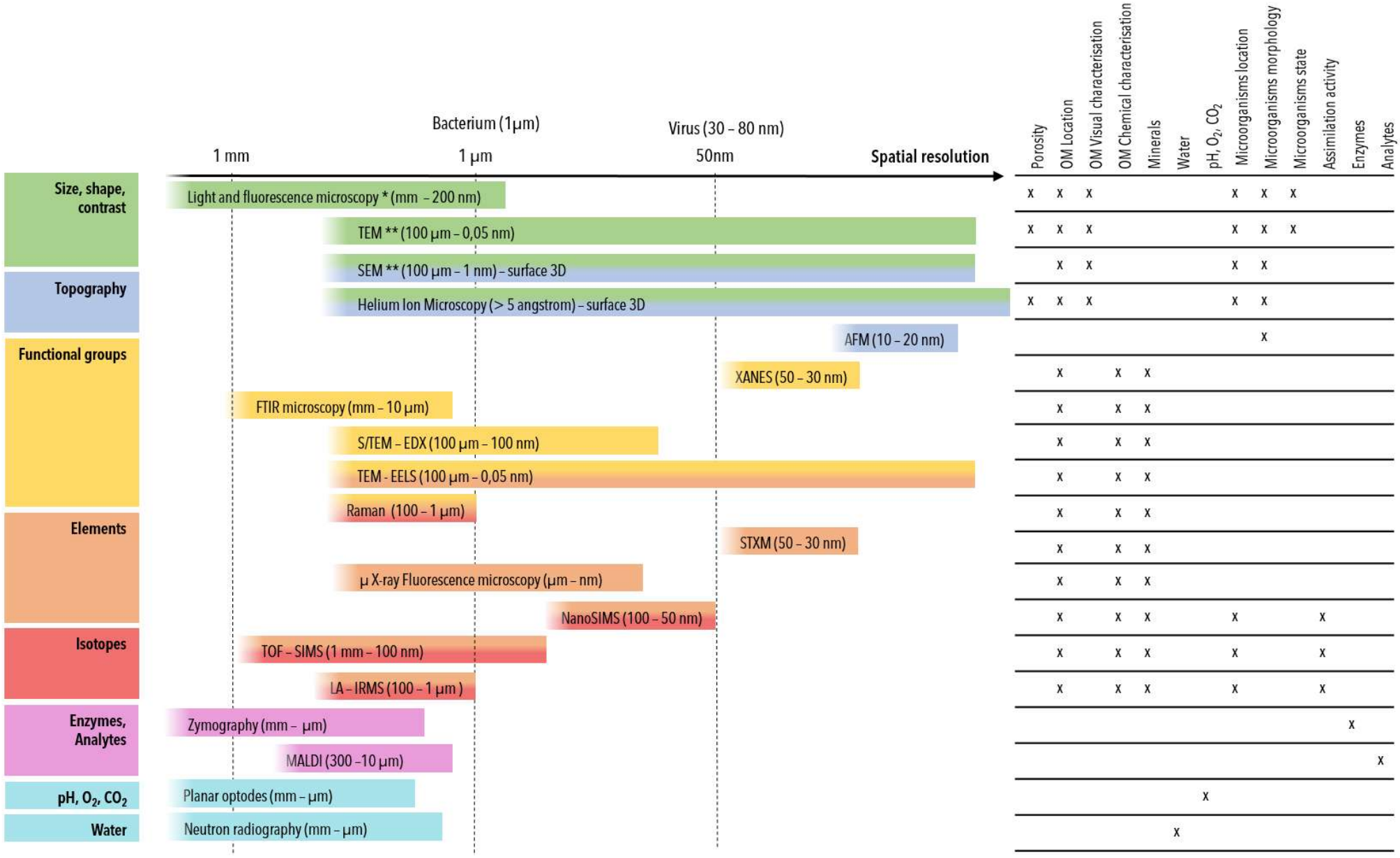

Fig. 1. 2D imaging methods organised depending their spatial resolution range possibilities and according to the information given by the produced images.
* In fluorescent microscopy stains (fluorochromes, FISH, BONCAT) are added increase contrasts and differentiate microorganisms or OM from the background.
** In electron microscopy, contrast agents (gold-FISH, osmium, iodine) are added to increase the contrast and differenciate microorganisms or OM from the background.

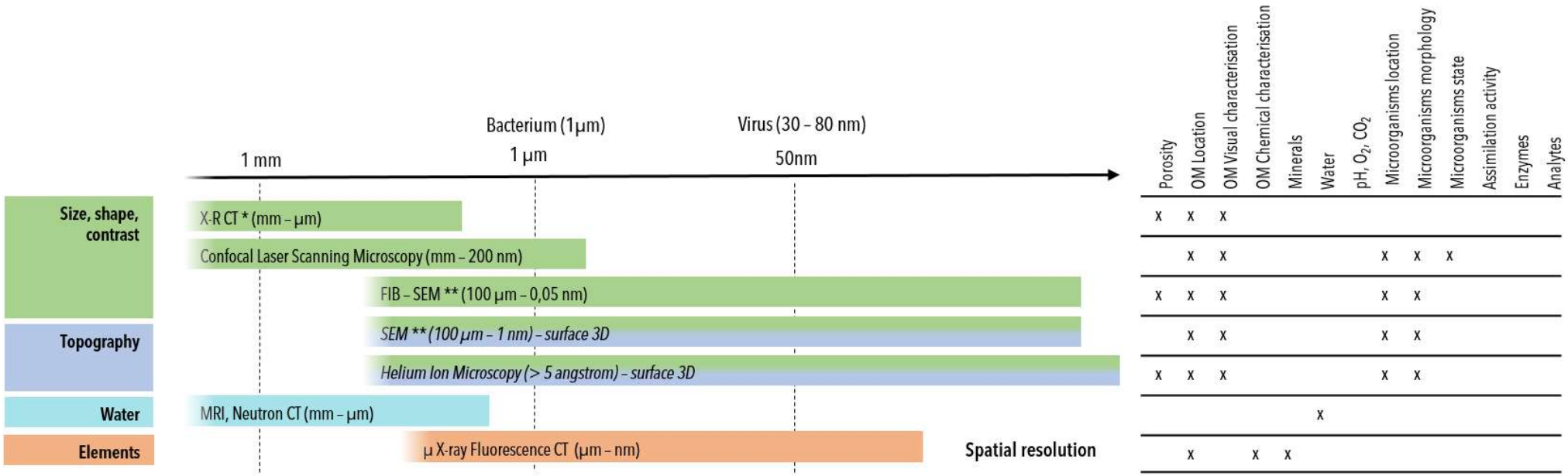

Fig. 2. 3D imaging methods organised depending their spatial resolution range possibilities and according to the information given by the produced images.
* In X-ray computed tomography contrast agents (osmium, iodine) can be added allowing increasing contrasts and differentiating OM from the background.
** In electron microscopy, contrast agents (gold-FISH, osmium, iodine) can be added to increase the contrast and differentiate OM from the background.

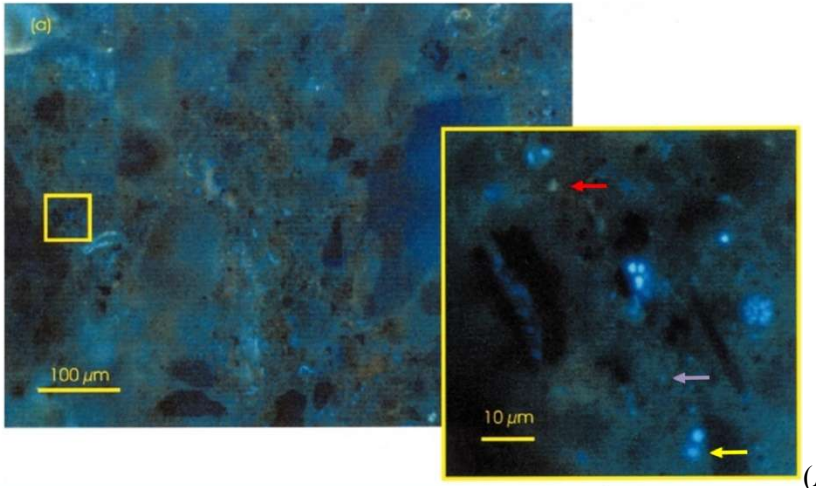

(A)

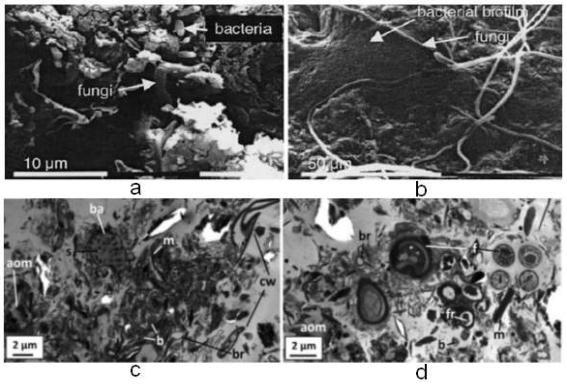

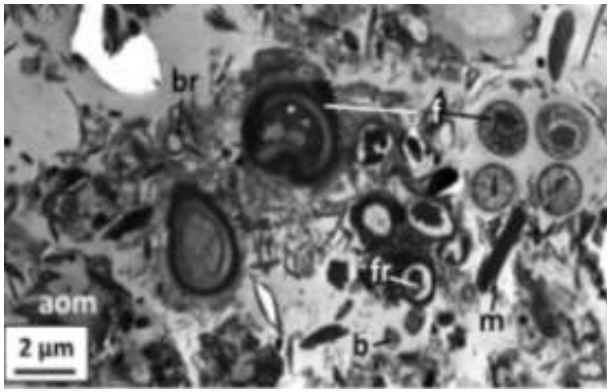

(B) (C)

Fig. 3. Example of methods allowing microorganisms visualisation.

(A) Composed image coming from different thin sections stained with CalcoFluor White and observed with an epi-fluorescence microscope. The yellow arrow indicates a bacteria identified by the image post processing, the red arrow indicates the presence of auto fluorescence and the purple arrow indicates an element too small to be clearly identified even with the post processing. Images: Nunan et al. (2001).

(B) Microorganisms observed, with SEM, at the surface of micro-aggregates of soil. Images: Chenu et al. (2001).

(C) Observations of microorganisms, with TEM, in bacterial aggregates soil after inclusion in a resin and preparation of ultrathin sections (aom: amorphous organic matter; b: bacteria; br: bacterial residue; f: fungi; fr: fungal residue; m: mineral). Image: Vidal et al. (2016).

(D, E, F and G) Microorganisms observations (Rhizobium leguminosarum strain on the rhizoplane of wetland rice, targeted by EUB338 probe and after staining with Gold-FISH technique under fluorescence microscopy (D), SE-images (E and F) and BSE-images (G). Scale bar : 20µm (D), 10 µm (E) and 1 µm (F and G). Images: Schmidt et al. (2012).

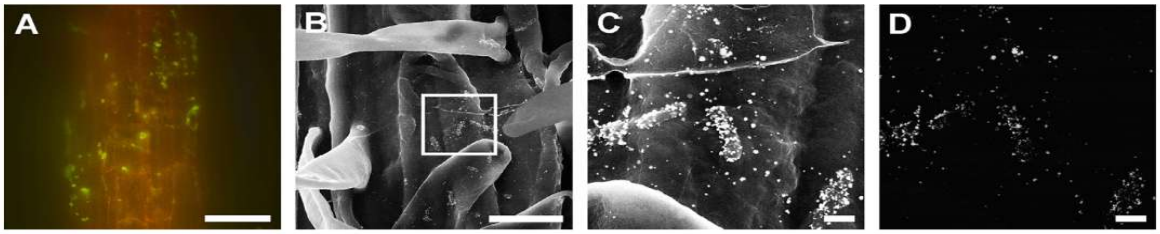

(D) (E) (F) (G)

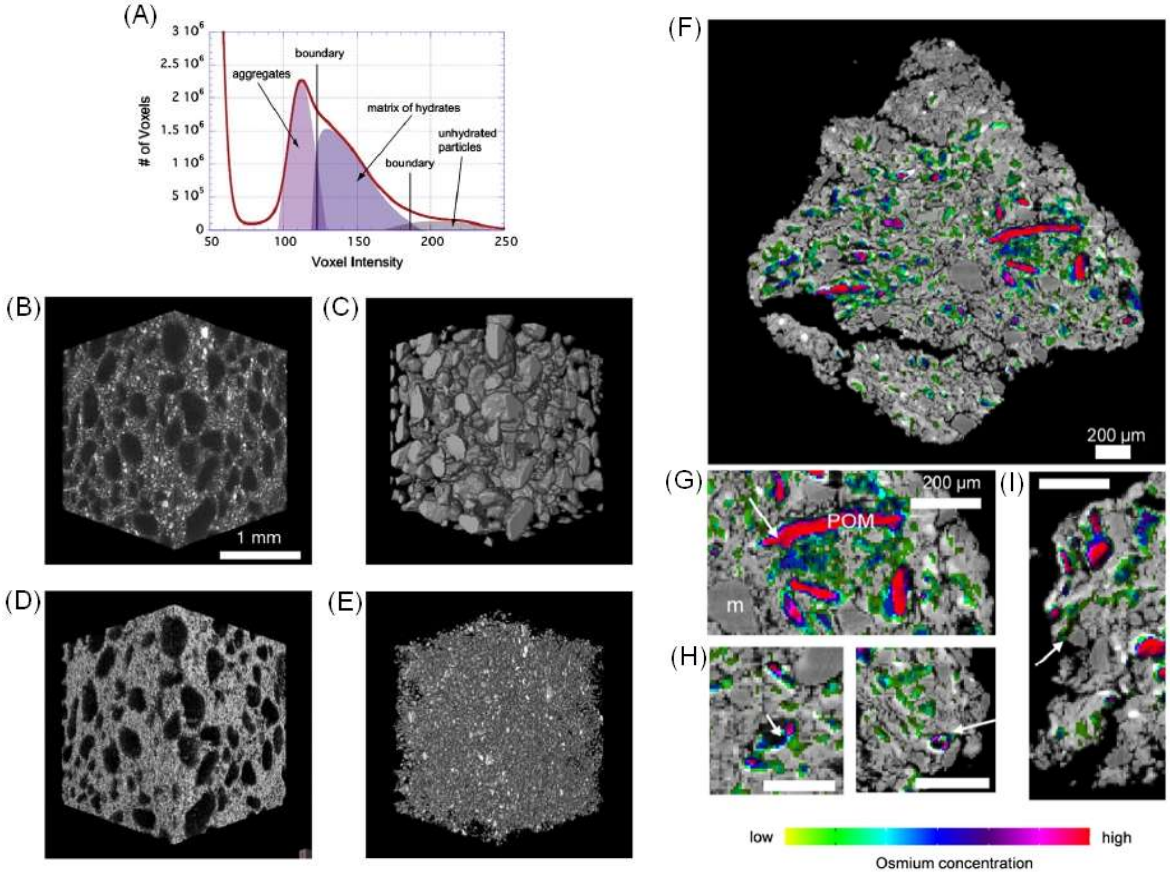

Fig. 4. Images obtained by X-ray tomography of a cement material (B) in which are segmented 3 solid phases: aggregates (C), cement hydrates (D) and un-hydrated particles (E) through the histogram of the image (A), the thresholds or boundaries of which are placed at the weakest points of the phase overlap. Images modified from Landis and Keane (2010).

Staining of OM with osmium inside a section of aggregate observed under synchrotron-based X-ray microtomography (F). Particulate OM (POM) show a strong osmium staining in red (G) and a less important staining in green at the pore surface (considered as pore coatings) (H) or following cracks (I). Images: Peth et al. (2014).

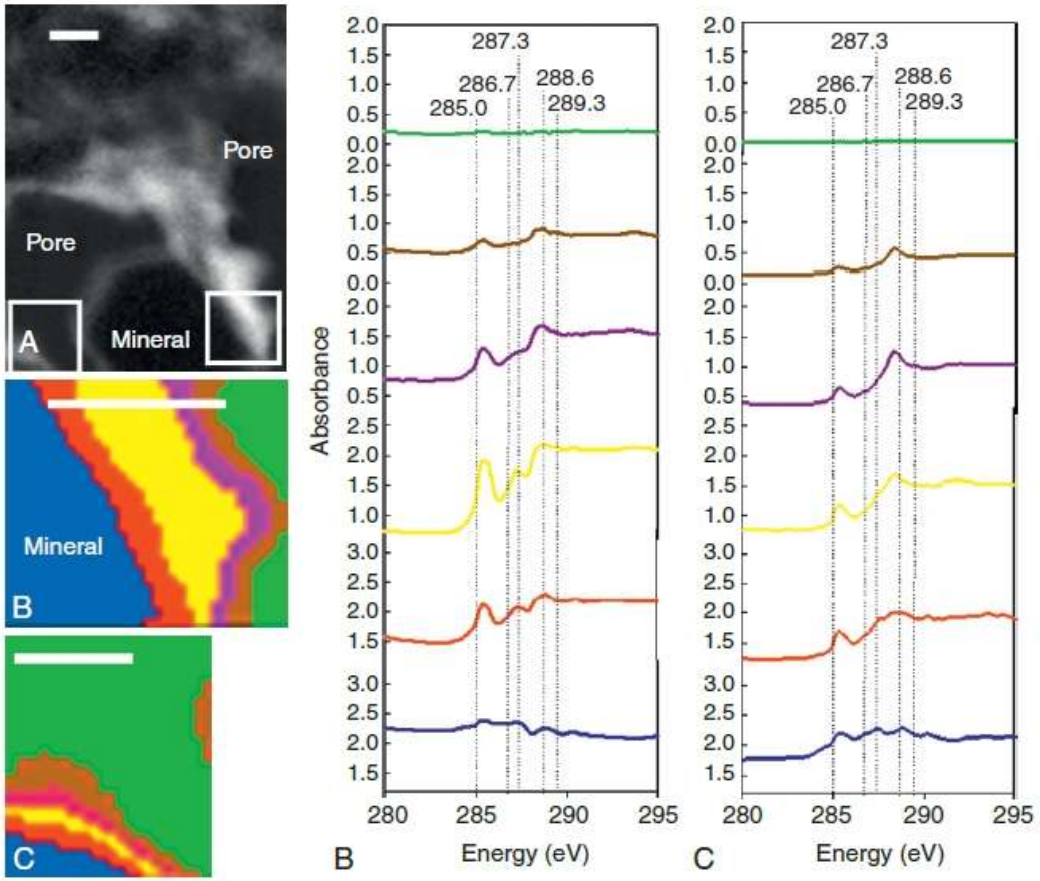

Fig. 5. Observations of organic carbon from a kaolin Oxisol by NEXAFS (resolution = 50 nm). (A) Optical density map of total carbon: light zones indicate the presence of carbon; white squares indicate interest zones on which the NEXAFS map had been done (B) and (C). Scale bars: 1 µm. Images: Singh and Gräfe (2010) from Kinyangi et al. (2006).

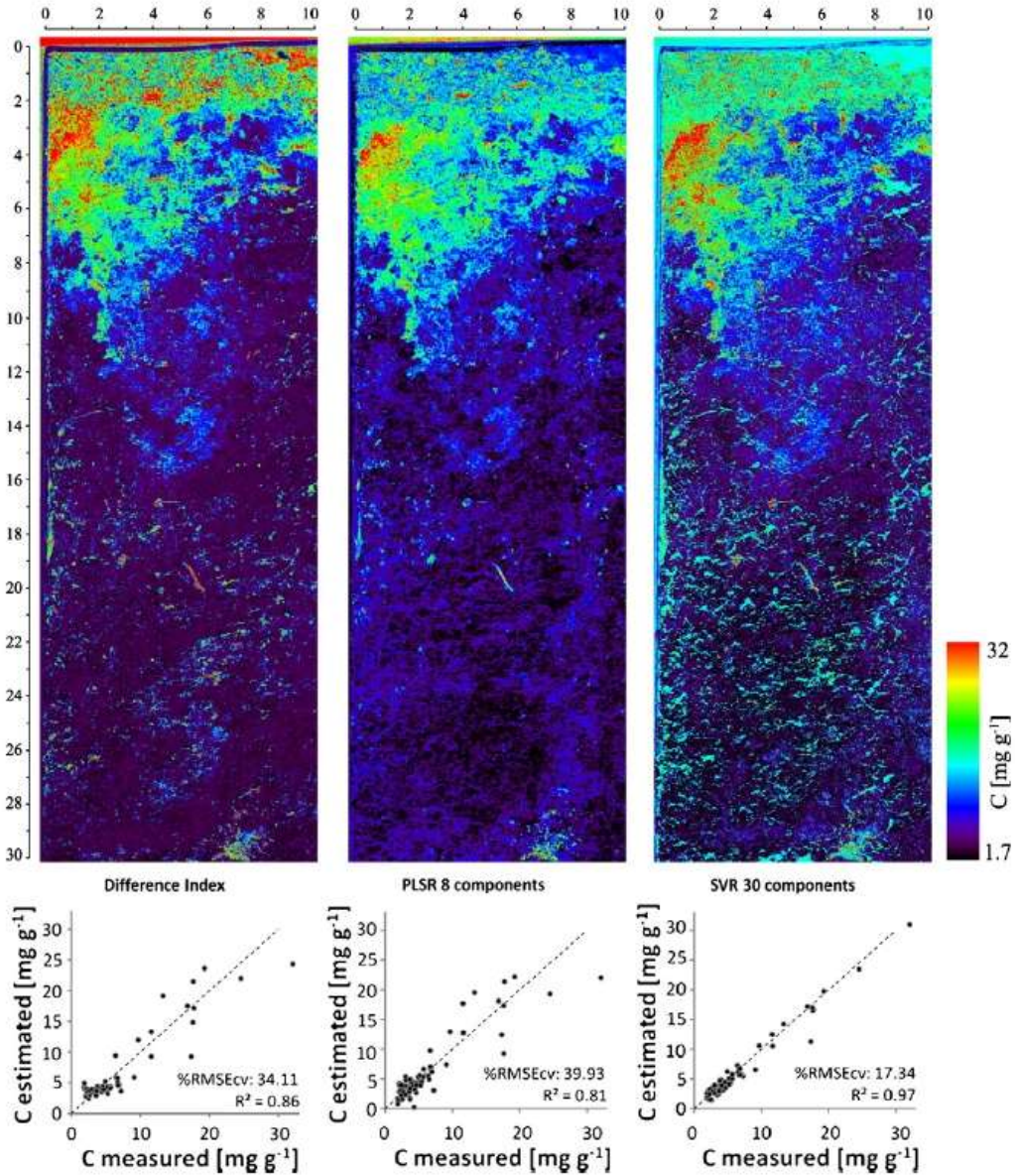

Fig. 6. Carbon concentration forecast and their repartition in a soil observed with hyperspectral VNIR camera and 3 linear regression models (narrow band index, partial least square regression (PLSR) and support vector regression (SVR)) – Dimension of soil samples: 10×30 cm. Images: Steffens and Buddenbaum, (2013)

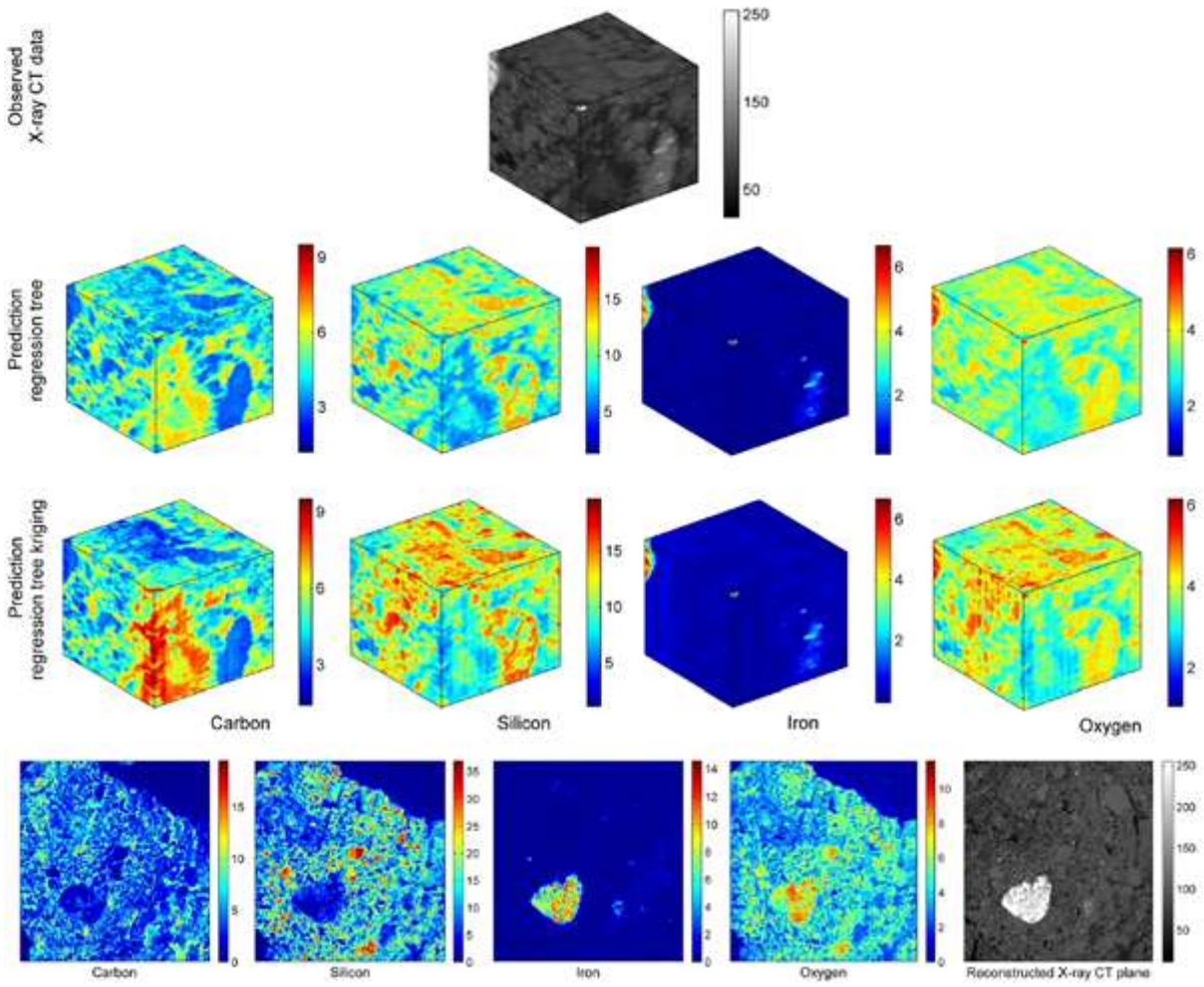

Fig. 7. Chemical maps of carbon, silicon, iron and oxygen obtained with SEM-EDX combined with X-R CT allowing getting a 3D reconstruction of soil chemical composition using a statistical approach with a regression tree and a krigeage regression tree. Each cube measure approximatively 1 x 1 x 1.3 cm. Images from: Hapca et al. (2015).

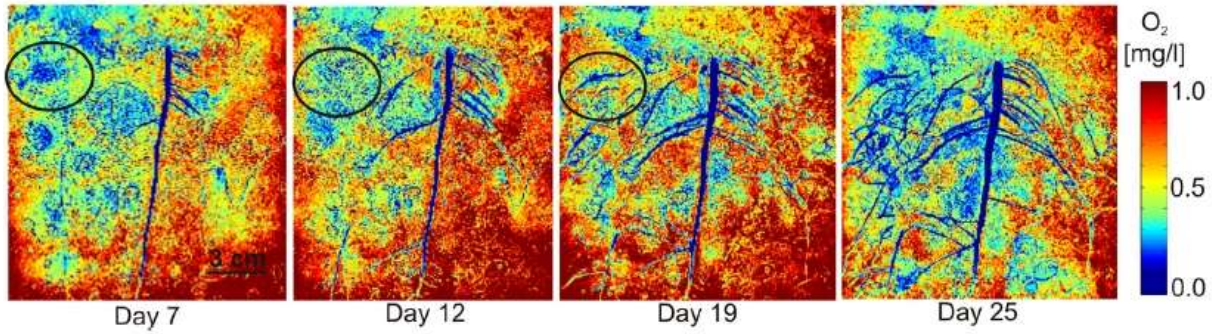

Fig. 8. Images taken over time with the use a chemical probe of the evolution of O_2 induced by the respiration of lupine roots. Images from Rudolph et al. (2012)**.**

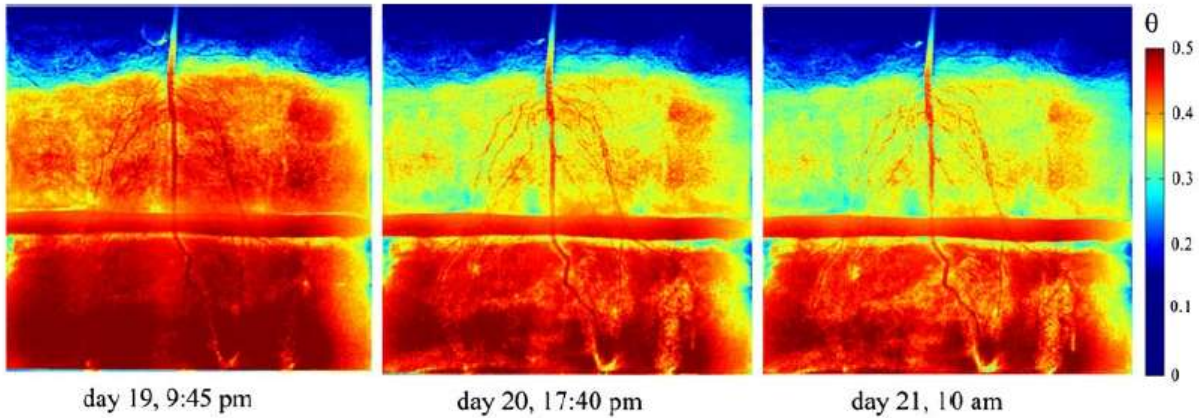

Fig. 9. Images realised with neutron radiography showing the distribution of water around lupine roots in sand. Each image measures 10 x 10 cm approximatively. Images from: Rudolph et al. (2012).

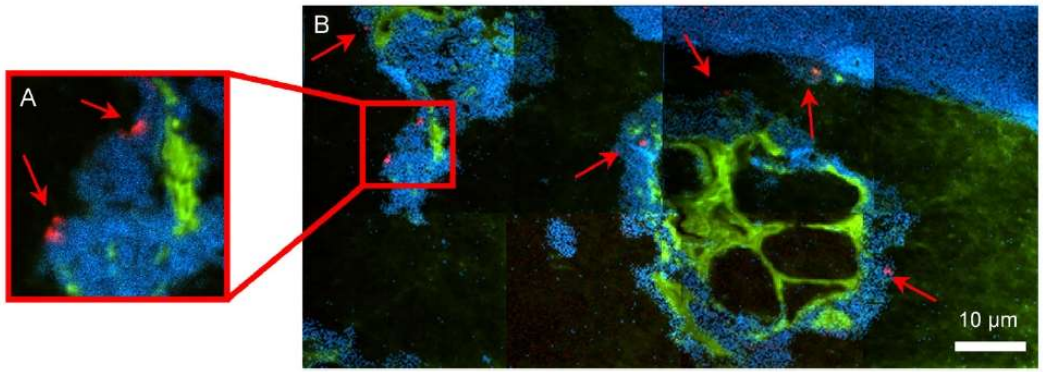

Fig. 10. Section of a *Pseudomonas fluorescens* colony in a soil after addition of ^{15}N. The cells that have assimilated the ^{15}N are visualised in red. (A) sur-imposed NanoSIMS images (in blue:$^{28}Si^-$, in green: $^{12}C^{14}N^-$ and in red: ratio $^{15}/^{14}N$). (B) Mosaic of superimposed NanoSIMS images following the same caption. Red arrows indicate *Pseudomonas fluorescens* labelled in soil. Images: Herrmann et al. (2007b).

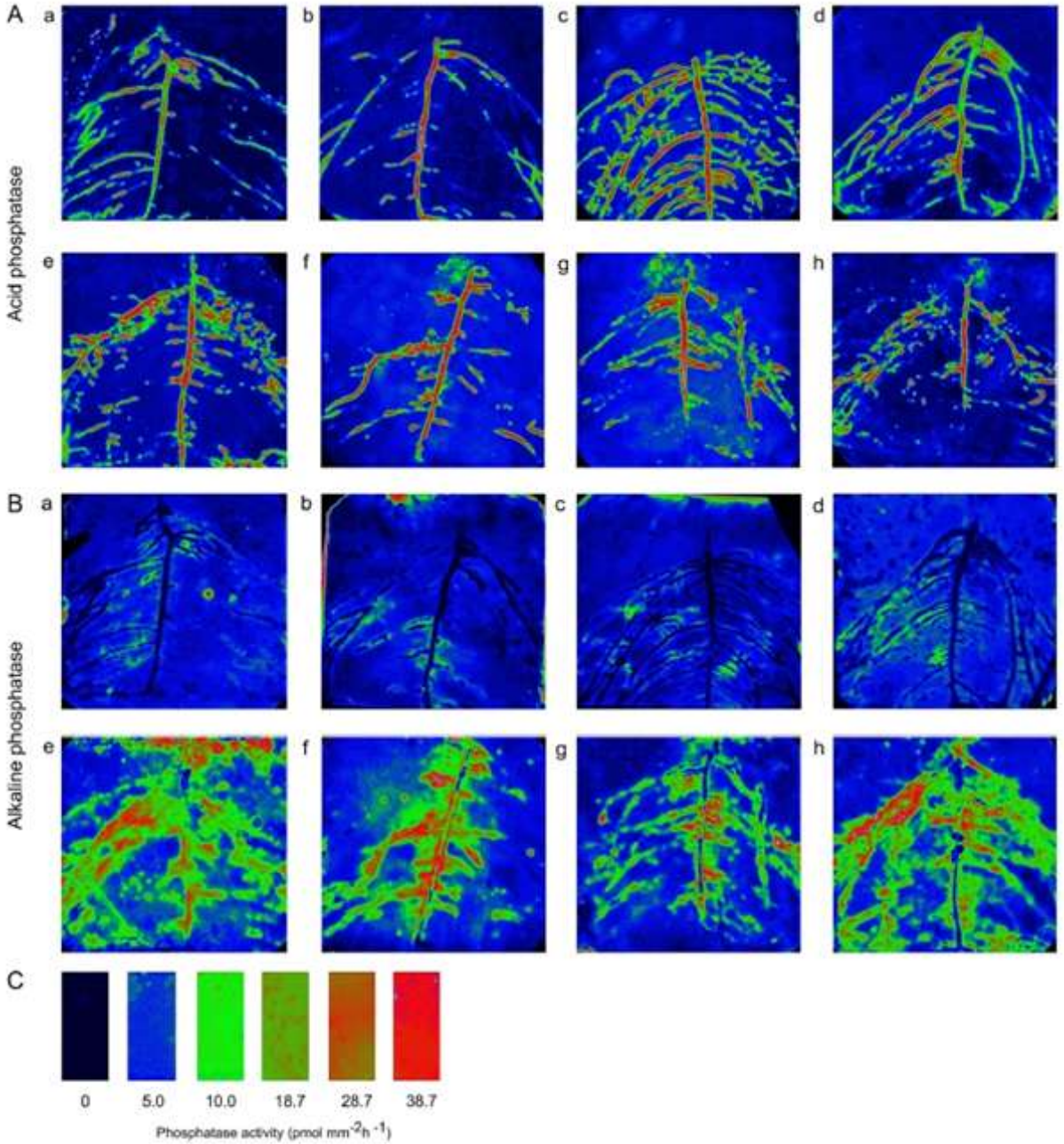

Fig. 11. Zymograms showing the activity of phosphatase enzyme around a root system in an amended soil (a, b, c, d) and control soil (e, f, g, h) with (A) acid phosphatase enzyme and (B) alkaline phosphatase with (C) as calibration membranes. Each image measure 12 x 11 cm. Images : Spohn et al. (2013).